Modern Applied Science
www.ccsenet.org/journal.html
Vol. 3, No. 5
May 2009

Optimization of the Technology of Wire Drawing Based on Finite Element Modeling

Gui'e Xu
School of Architecture Engineering
Nantong University
Jiangsu, China
Tel: 86-513-8501-2655 E-mial: xuge@ntu.edu.cn
Feng Fang
College of Material Science and Engineering
Southeast University
Jiangsu, China
Zhaoxia Li
College of Civil Engineering
Southeast University
Nanjing, Jiangsu, China

Abstract

The initiation and propagation rule of central flaw during wire drawing was modeled with the finite element method and theory of fracture mechanics. It is shown that: J-integral value increased with the increasing of the angle of drawing die, the friction coefficient between drawing die and wire and the initial dimension of the flaw. When friction coefficient equaled 0.1, J-integral value round the crack tip with the same flaw decreased with the decreasing of the angle of the die. J-integral value changed slightly and tended to be a constant value when the angle reached to 8°. The calculated results were then applied to improve the optimization of the technology for wire drawing.

Keywords: Drawing, Steel wire, Central flaw, Critical size, J-integral value

Wire drawing, an important means of cold forming process of forming, has received a wide range of applications in the production. Wire drawing process is very complex material deformation process, has many impact factors. Not only has material organizational changes (including the organization of deformation, the formation of micro-texture, etc.), also includes the process of drawing rod temperature, surface condition changes. Their drawing process, the deformation of the wire in the drawing process is mainly affected by four factors, die angle of the mold, the friction coefficient between materials and the mold, area shrinkage rate and hardening coefficient (Avitzur. B, 1968)(Z. Zimerman, and B. Avitzur, 1970)(Yu Wanhua, Huan Guanchang, Yuan Kang, 1994)(J. Luksza, J. Majta, M. Burdek, et al. 1998)(R. K. Chin, P.S. Steif, 1995). Configuration of these factors is reasonable or not drawing a direct impact on the quality of the process. Unreasonable configuration parameters are usually makes the formation of the core wire break or even crack in wire drawing process. High rate of broken wires in drawing has been an issue of great concern in the production.

A lot of study has been done about the deformation of materials in wire drawing process. Zimerman and Avitzur (Avitzur. B, 1968)(Z. Zimerman, and B. Avitzur, 1970) studied the effect of strain hardening on central bursting defects in drawing and extrusion. YU Wan-hua etc. (Yu Wanhua, Huan Guanchang, Yuan Kang, 1994) calculated the security zone map in which the core cracks are prevented. Luksza (J. Luksza, J. Majta, M. Burdek, et al. 1998), Chin (R. K. Chin, P.S. Steif, 1995), Ko (Ko. Dae-Cheol, Kim.Byung-Min, 2000), Komori (Kazutake. Komori, 2003) also took some numerical simulation analysis on the material deformation state in drawing process. These numerical simulation analyses may be effective, but the complexity of calculating was burdensome, and does not take into account the materials deformation state after crack initiation. In recent years, based on the finite element method of calculation software was perfect, powerful and fast, people could use it to optimize production or production process. In this paper, crack initiation stage was neglected; influence of existent cracks to the deformation in wire drawing was focused on. It has a study of the evolution of crack in the deformation region and explores the impact of parameters in wire drawing on the evolution of the department of core crack in the process, such as the friction coefficient, mold angle, etc. Assuming the pass rate of contraction, hardening coefficient unchanged.

1. Analysis model of wire drawing process with a central flaw

Consecutive 8-time drawing is widely used for wire drawing process today. This paper takes a production line of 8 molds as the research object, in which a steel rod with an initial diameter of 13mm is drawn to a final diameter of 5.3mm. Material work hardening is occurred after each drawing, so the plastic of the material are reduced. With the increase of drawing time, the impact of residual strain to the rod is more serious, resulting in a more vulnerable expansion of crack in the final 1 or 2 pass, and even broken. So the study to this article dominates the deformation and crack evolution of the rod in the final pass. In order to simulate the possible internal defects may formed before the rod began its eighth drawing, firstly, defects in product are observed on the draw bench of a production line.

1.1 Observation of Internal Defects in Drawing Wire

Checking the results of samples coming from the production line may observe a certain proportion of the drawing fracture which named Nib-shaped fracture, the morphology of which shown as Figure 1 (a), which account for a certain number of broken wires rate. The shape of the fracture looks like a sharpened nib as observing from the drawing fracture sample photos. Such a fracture is formed from the expansion of the instability of a central defect by metallographic study, see Figure 1 (b). In this longitudinal profile of material containing inner cracks a sharpen-nib crack has formed. If this crack continues to expand, the fracture morphology ultimately will be as shown as Figure 1 (a).

The formation and expansion of central cracks is complex. On the one hand, the material deformation of the outer layer is not consistent with that of the inner layer, with a smallest deformation in the core. On the other hand, the material itself contains central defects. Combination of those two factors results in a materials failure launch easily from the central defects, firstly, that is, the formation and propagation of the crack even fracture. Ignore the complexity of defects, the simplest calculation model of the process of drawing is based on the assumption rod containing a disc-shaped initial central defect. And ignore the impact of the entrance and sizing of the mold, only take the role of cone deformation into account.

1.2 Mechanical Properties of Drawing Wire

Mechanical performance parameters of the drawing wire used in the simulated calculation are measured by standard experiment (Wang Zhutang, Guan Yandong, Xiao Jingrong, et al, 1989). According to the measured results, the material's true stress - strain curve is measured by extrapolation. Fracture toughness J_{IC} (J-integral value) is measured by single-sample method with standard specimens. Take conditional yield strength $\sigma_{0.2}$ in unidirectional tensile test stress - strain curve as initial yield strength. Other yield strength is obtained by the extrapolation of stress - strain curve. Drawing forces are calculated with approximate formula (Wang Zhutang, Guan Yandong, Xiao Jingrong, et al, 1989) as following:

$$\sigma_r \approx \sigma_s \left[\left(1 + \mu ctg\alpha\right) \ln \frac{A_1}{A_2} + \frac{4\alpha}{3\sqrt{3}} \right] \tag{1}$$

The change of corresponding material parameters, such as the material's yield strength after drawing, and the technical parameters (all-pass response, drawing force, mold length) are the light of the actual value of production. Other material parameters determined by experiment, in that, elastic modulus $E = 210GPa$, Poisson's ratio $\nu = 0.25$.

1.3 Analysis Models of Drawing Wire

In the simulation of the eighth drawing pass, the residual strain generates before is negligible. Due to the symmetry, the problem can be simplified by setting up finite element model with axial symmetry unit, and assuming the defect is located at the center of the rod. Take that a simulation can only take a limited length and that the state of deformation should be as far as possible near the actual line both into account, the rod aspect ratio check (axial length / radius length) ≥ 5, the ratio of rod length to initial crack size (axial length / 2a) ≥ 10 are used in the simulations. The finite element model of drawing wire set up with commercial software ANSYS and meshing near the crack tip are shown in Figure 2.

2. Simulation of the Forming Process of a Fracture

2.1 Analysis on the formation of a Nib-shaped fracture

Drawing from the aforementioned shortcomings within the sampling test results of the production line, we can see that in the observed fractures certain amounts of fracture are nib-shaped. The formation of Nib-shaped fracture is originated in the core defects in material. Stress concentration is occurred in the drawing stress state, and with an orientation obtuse with the drawing direction. When the defect size is bigger than critical size, the crack will expand gradually along the direction of the largest stress concentration, until a chevron crack forms. When the crack growth to a certain size it expands unstably and rapidly until the fracture formed, with the formation of a smaller shear lip in the final expansion stage. Fracture is nib-like: that is, the source region of crack, the symmetrical expansion zone of crack and the shear lip zone. Its formation process diagram is shown in Figure 3.

2.2 Simulation to the formation of a Nib-shaped fracture

Assuming no defects exist in the rod. A model is set up to simulate the wire drawing process of a Defect-free rod. The simulation showed that in the central location of the export of the Wire Drawing Die there achieves a smaller compressive stress and a larger axial tensile stress. These two stress combine to effect, resulting in a maximum stress in the export position. As the actual material is always uneven, and therefore, material in the center of the rod is more likely produce micro-cracks in wire drawing. In order to explore the mechanical causes of the formation of Nib-shaped fracture, based on this stress field further analysis and simulation is made to study internal stress distribution and stress concentration in crack tip with a central defect. In the first pull-out, the rod has not been strain-hardening and has good internal mobility. As the first pull-out is also the starting point of the internal non-uniform strain of the rod, the deformation in this drawing has been the best point of observing the trend of further deformation in material. So we observe the deformation trends of drawing wire in its first pull-out processes, while the study on internal stress distribution and stress concentration in crack tip after cracks is exist is based on the finial pass.

By the method described in 1.3 finite element models are set up to simulate drawing wire in Road 8(see Fig.2) and are used to study the stress concentration state around crack tip. Finite element analysis results shown in Figure 4 and 5 are stress distribution around crack tip when central defect is passing the mold-outer, when the rod bear a large deformation and stress concentration around crack tip has been serious. In the deformation zone of the mold, compression stress is mainly in radial and tensile stress is mainly in axial. While the crack growth mainly caused by the role of the tensile stress, there only shows axial stress distribution cloud, see figure 4. Figure 4 (a) is the axial stress distribution cloud, Figure 4 (b) is axial stress concentration around the crack tip. As shown in Figure 4(a) stress in axial is mainly tensile when the rod passing the die, with a larger stress near the crack and gradually decreased stress away. There is a clear stress concentration around the crack tip, and slightly away from the crack tip, stress concentration orientation has an obtuse angle to the drawing direction, as shown in Figure 4(b). According to this phenomenon, the process of crack growth can be described as, firstly the defect has a slight expansion with the vertical drawing direction, and then turns into a obtuse angle with the drawing direction. The calculation results are coincided with the actual observed experimental results (Fang. Feng, 2003).

2.3 The Impact Factors of Nib-shaped Fracture

Research on Nib-shaped fracture can help to determine the main reasons for the occurrence of broken wires in wire drawing, and from the location of material defects the defects in the original materials and the causes why they occur may be inferred, contributing to the improvement of rod production process and enhance their quality, and optimize the drawing process parameters.

There are many factors impact the morphology of Nib-like fracture, including the material performance parameters, the size of die angle in drawing, lubricant condition, the drawing rate, cooling conditions, where the research is focused on the impact of drawing angle of the die and lubrication to the morphology of nib-like fracture. Changing die angle in wire drawing, other parameters are unchanged. The results show that, with the wire drawing die angle increases, the oblique angle of nib-shaped fracture also become larger, that is, the nib become more slender. Change the friction coefficient between the drawing with the die, from $\mu = 0.1$ to $\mu = 0.3$, other parameters unchanged. The results showed that with increasing friction coefficient, the oblique angle of nib-shaped fracture is also smaller, i.e. shorter nib.

3. The Critical Size of Central Defects

For further quantification of the impact of process parameters to the crack tip stress field, such as die angle, friction coefficient, J-integral around crack tip are calculated with the simulation results of the ANSYS finite element models, which are based on the drawing road 8.

3.1 Relationship between J-integral and the die angle

Change the die angle with other process parameters unchanged, the J-integral values for two crack sizes (2a = 20μm and 50μm) are obtained, here with . The relationship curves between J-integral value and the die angle are shown as Figure 6 (a), in which the dotted line charts for the experimentally measured values JIC of the material. From the figure, we can see that changes of J-integral with the die angle-size for different crack size are basically the same. J-integral value also increases along with the increase in crack size. For the same size of the crack, J-integral value decreases as the die angle decreases until it get to a boundary, when J-integral value changes slightly and tends to a certain value, here about 8 °.

From the above analysis we can see that smaller die-angle in wire drawing reduces the tendency of crack propagation. It is unsuitable for very small angle dies used in actual production process, as the need to consider the design and manufacture of molds, energy consumption in the process of drawing, productivity and other factors. Other settings unchanged, trades-off between the finished product quality and efficient pull-out, a die angle that both ensure a high area compression ratio and also greatly reduce the of crack propagation can be obtained, that is the best pulling angle. For the production of wire drawing, as the friction coefficient μ is about 0.1, the best pulling angle is about 8 °. With this die angle, the permitted defects within materials can have a relatively larger value, that is, brings a lower rate of broken wires in wire drawing.

3.2 Relationship between J-integral and crack size

Change the crack size with other process parameters unchanged, the J-integral values by the condition of the friction coefficient (μ) of 0.1 and 0.3 are obtained, here die angle 2α = 8 °. The relationship curves of J-integral values to micro-crack size are shown as Figure 6(b), in that the dotted line charts for the JIC value of the material. It can be seen from Figure 6(b) that J-integral value increases with the increase in crack size, and under the same initial defects J-integral value is slightly larger with a larger coefficient of friction. The critical defect size is between 30μm and 40μm from the map also under the two cases of friction coefficient. The friction coefficient of actual process is of approximately 0.1 and observed critical crack size under this case is about 30μm. This shows that simulation results are close to the actual situation.

3.3 Relationship between J-integral and friction coefficient

Now we take the case of die angle 2α = 8 °, and other process parameters unchanged, only with changing friction coefficient. The J-integral values are obtained for two different defect sizes (20μm and 50μm). The relationship curves of J-integral value to friction coefficient are shown as Figure 6(c). From the figure we can see that J-integral value increases with the increasing of friction coefficient. The greater the friction coefficient, the greater the J-integral value for the same initial defects. This is because the friction coefficient decreases causes a reducing friction, shear stress also decreases. As a result, the extent of stress concentration around crack tip decreased, corresponding J-integral value is also reduced.

4. Optimization analysis on the drawing process Based on the simulation results

Based on the above simulation and analysis results, for the pull-out production process with high carbon wire, we can draw the following advice:

For the same size of the crack, J-integral value decreases as the die angle decreases, until the later reach some certain boundary J-integral value changes in smaller, the certain value of die angle here is about 8 °. Analysis showed that smaller die angle in wire drawing reduces the tendency of crack propagation. However, in order to ensure higher productivity, die angle also should not be too small. With improved friction performance friction coefficient μ in actual production is usually about 0.1, the best pulling angle is 8° or so for this case of friction coefficient. With this die angle, the permitted defects within materials can have a relatively larger value, that is, brings a lower rate of broken wires in wire drawing.

With the increase in friction coefficient, J-integral value increases; the greater the friction coefficient, the greater the J-integral value for the same initial defects. Thus, improving lubrication conditions of the drawing process means larger critical crack size in materials, in other words, brings a lower rate of broken wires in wire drawing.

With the best framework of process parameters, certain size of central initial defects in rod is permitted that will not expand in drawing, namely, the critical crack size. The critical size of central defects identified in this study is of 30-40μm.

It is of great significance for the effectiveness of the production if we can carry out nondestructive testing in the rod to control the rod's quality before the drawing, by ensuring the quality of finished products at the same time saving materials.

5. Concluding Remarks

In this study, we benefit with the use of large-scale commercial software ANSYS and fracture mechanics theory for simulation of evolution law of defects in metal wire drawing process, as well as the impact of control parameters in the drawing process on the evolution of defects. Study on stress and strain field distribution in deformation zone with defect-free rod gives a verification of the formation mechanism of core chevron crack. As a result of rod material containing defects or drawing effects of several times before, the probability of crack expansion in the final two or one drawing has been great in multi-pass drawing, four factors have impact on the crack evolution; we use the finite element software to calculate the impact of friction coefficient and die angle on the evolution of cracks, then rational configuration is taken to adjust these factors for the purpose of reducing broken wires rate in its pull-out. It is concluded that the friction coefficient is 0.1 and the best pull-out angle is of approximately 8° and the rate of broken wires can be reduced by improving the lubrication conditions in wire drawing; While the diameter of the disc-shaped surface crack in the central of the rod is no more than 30-40μm, the wire break will not happen.

References

Avitzur. B. (1968). Analysis of central bursting defects in extrusion and wire drawing. *Transactions of the ASME Journal of Engineering for Industry.* 1968, 90 (1): 79-91.

Fang. Feng. (2003). The performance and microstructure of 1860Mpa PC strand produced by little billet continuous casting hot continuous rolling. In: *Department of Material Science and Engineering of Southeast University*, NanJing, 2003.

J. Luksza, J. Majta, M. Burdek, et al. (1998). Modeling and measurements of mechanical behavior in multi-pass drawing process. *Journal of Material Processing Technology*, 1998, (80-81): 398-405.

Kazutake. Komori. (2003). Effect of ductile fracture criteria on chevron crack formation and evolution in drawing. *International Journal of Mechanical Sciences*. 2003(45): 141-160.

Ko. Dae-Cheol, Kim.Byung-Min. (2000). The prediction of central burst defects in extrusion and wire drawing. *Journal of Material Processing Technology*. 2000, (102): 19-24.

R. K. Chin, P.S. Steif. (1995). Computational study of strain inhomogeneity in wire drawing. *Int. J Mach Tools Manufact*. 1995, 35(8): 1087-1098.

Wang Zhutang, Guan Yandong, Xiao Jingrong, et al. (1989). *Theorems of plastic metal forming*. BeiJing: public of mechanical industry. 1989: 165-167.

Yu Wanhua, Huan Guanchang, Yuan Kang. (1994). Criterion for central bursting in wire during drawing. *Journal of University of Science and Technology* BeiJing, 1994, 10(2): 162-165.

Z. Zimerman, and B. Avitzur. (1970). Analysis of the effect of strain hardening on central bursting defects in drawing and extrusion. *Transactions of the ASME Journal of Engineering for Industry*. 1970(2): 135-145.

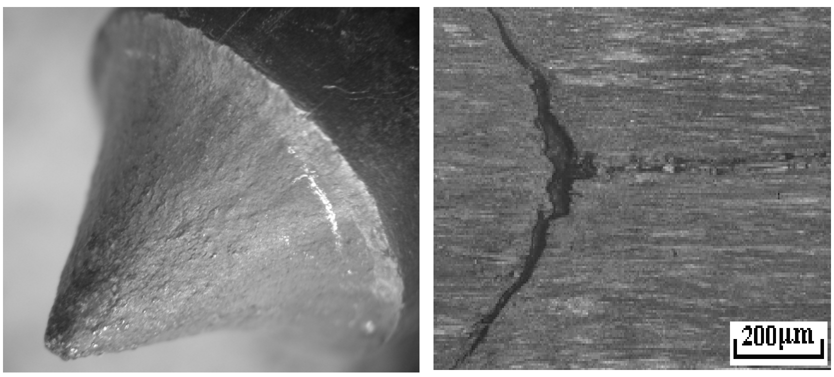

(a) Fracture surface (b) vertical profile

Figure 1. Morphology of drawing fracture

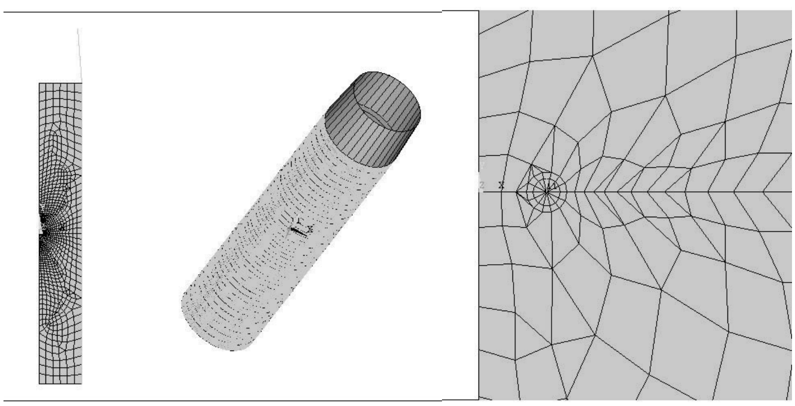

(a) Axial symmetry plane model (b) Axial symmetry model of the entire expansion (c) mesh near crack tip zone

Figure 2. Finite element model of drawing wire

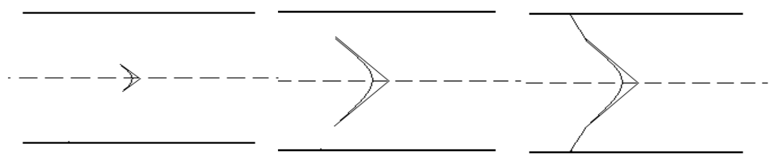

(a) Crack source; (b) expansion period; (c) period of fracture

Figure 3. Sketch map of nibbled pencil fracture formed

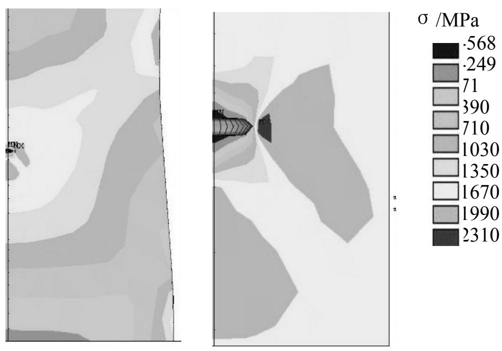

(a) Axial stress (b) stress concentration around crack tip

Figure 4. Nephogram of stress distributing in drawing mold (axial stress)

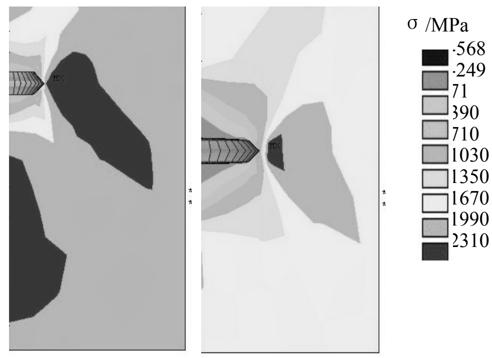

(a) $2\alpha=30°$ (b) $\mu=0.3$

Figure 5. stress concentration

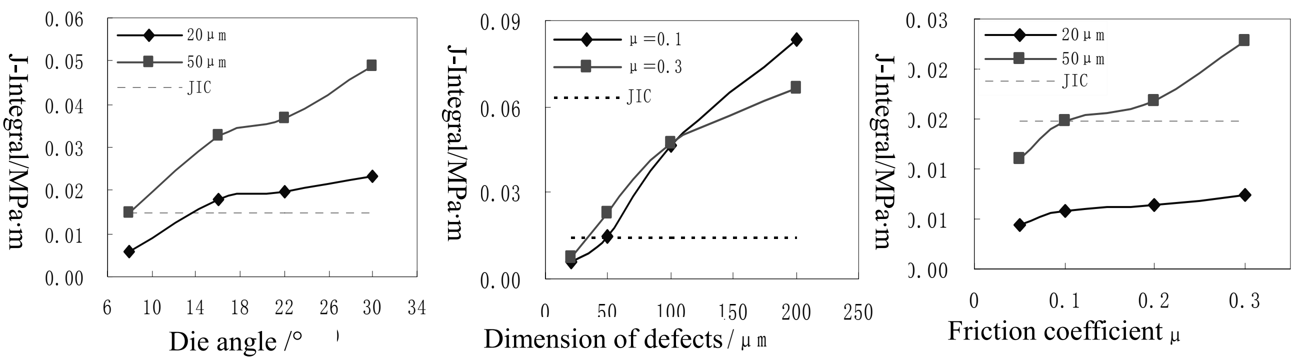

(a) J-Integral *versus* apex angle (b) J-Integral *versus* the dimension of defects (c) J-Integral *versus* friction coefficient

Figure 6. the relationship between J-integral and the die angle, crack size and friction coefficient